ACADEMIC
PRESS

Synthesis and crystal structure of the monoclinic modification of Yb(ReO$_4$)$_3$(H$_2$O)$_4$

Carlos Mujica,[a,*] Jaime Llanos,[a] Víctor Sánchez,[a] Pedro Gómez-Romero,[b] and Nieves Casañ-Pastor[b]

[a] *Departamento de Química, Universidad Católica del Norte, Angamos 0610, Casilla 1280, Antofagasta, Chile*
[b] *Institut de Ciència de Materials de Barcelona, (CSIC) Campus UAB, Bellaterra 08193, Spain*

Abstract

Ytterbium(III) tetraaquatris(tetraoxorhenate(VII)), Yb(ReO$_4$)$_3$(H$_2$O)$_4$, was prepared by the reaction of Yb$_2$O$_3$ with concentrated HReO$_4$ at room temperature. The colorless compound crystallizes in the monoclinic space group $P2_1/n$ (No. 14) with four formula units per unit cell ($a = 730.5(1)$ pm, $b = 1484.1(5)$ pm, $c = 1311.7(2)$ pm, $\beta = 93.69(1)$). The main feature of the crystal structure is the formation of chains $^1_\infty$[Yb(H$_2$O)$_4$(ReO$_4$)$_2$(ReO$_4$)$_{2/2}$] running along [100]. This arrangement shows distorted cubic antiprisms of [Yb(H$_2$O)$_4$(ReO$_4$)$_2$(ReO$_4$)$_{2/2}$] interconnected via the ReO$_4^-$ ligands. The chains are held together in the solid by hydrogen bonding. The compound is paramagnetic and follows the Curie–Weiss law with a magnetic moment of 4.0 μ_B at room temperature and $\theta = -42$ K. It loses hydration water in two steps at temperatures below 400 K; decomposition begins at 850 K, forming Yb$_2$O$_3$(Re$_2$O$_7$)$_2$ and is complete at 1350 K leading to Yb$_2$O$_3$ as final product.
© 2003 Elsevier Science (USA). All rights reserved.

Keywords: Ytterbium; Rhenates; Hydrates; Low-temperature synthesis; Crystal structure; Thermogravimetry; Magnetic properties

1. Introduction

Tetraoxorhenate(VII) complexes of transition elements as well as of the rare-earth cations are good examples how the ionic radii of the central ions determine the coordination number as well as the geometry of the complex. In previous papers, we have reported the synthesis and crystal structure of several such complexes. The small divalent cations of the first row transition metals [Fe, Co, Ni and Cu] form octahedral complexes coordinated by two ReO$_4$ ligands and four water molecules [1–5]. The slightly larger Mn(II) is coordinated by two water molecules and four tetraoxorhenate(VII) anions, which also act as bridge ligands connecting the complex into a chain $^1_\infty$[Mn(H$_2$O)$_2$(ReO$_4$)$_{4/2}$] [6,7]. The larger La(III), Eu(III) and Gd (III) ions are ninefold coordinated by three water molecules and six ReO$_4^-$ ligands, and these units are interconnected by the tetraoxorhenate(VII) anions to form three-dimensional networks [8–11]. The present

ytterbium compound was prepared in order to study the structural effects related to the ionic radii within the series of rare-earth elements. Given its smaller ionic radius, ytterbium can bridge the gap between smaller transition metals and larger lanthanides and thus provide a unique system for discerning the effects of size and chemical nature in the crystal–chemical construction of tetraoxorhenate structures. In this paper we report the synthesis, the crystal structure, thermal and magnetic properties of the title compound, ytterbium(III) tetraaquatris(tetraoxorhenate(VII)).

2. Experimental

2.1. Synthesis

For the synthesis of the title compound ytterbium oxide was slowly dissolved in perrhenic acid (HReO$_4$). The latter was prepared according to well-known methods by adding H$_2$O$_2$ (Merck, 30%) to solid rhenium powder (Aldrich, 99.9%) in an ice bath.

Table 1
Crystallographic data and details of the structure analysis

Formula; molar mass	$Yb(ReO_4)_3(H_2O)_4$; 995.72 amu
Crystal	Transparent colorless prism; $(0.1 \times 0.2 \times 0.25\,mm)$
Space group; formula units	$P2_1/n$ (No. 14); $Z = 4$
Unit cell (294 K)	$a = 730.5(1)$ pm
	$b = 1484.1(5)$ pm
	$c = 1311.7(2)$ pm
	$\beta = 93.69(1)$
Volume; density	$1419.1(4)\,\text{Å}^3$; $4.448\,\text{g cm}^{-3}$
Data collection	Enraf-Nonius CAD 4 four-circle diffractometer, MoKα radiation
	$(\lambda = 0,71073\,\text{Å})$; graphite monochromator, ω-scan mode, $2\theta < 60°$
Structure refinement	SHELX 93 SHELX 97 [11], direct methods, empirical absorption correction (ψ-scan method),
	$\mu = 32.11\,\text{mm}^{-1}$
Measured/unique reflections	4056/3799
Observed reflections ($F_o > 3.0\sigma(F_o)$)	1866
Weighting	σ^{-2}
R; Rw	0.054; 0.124

Table 2
Positional and equivalent displacement parameters U_{eq} (in pm^2). All atoms are at the Wyckoff position 4a

Atom	x	y	z	U_{eq}/U_{iso}
Re1	0.0345(1)	0.1422(1)	0.4371(1)	160(3)
Re2	0.9959(1)	0.2552(1)	0.7833(1)	126(3)
Re3	0.0498(1)	0.8742(1)	0.9129(1)	146(3)
Yb	0.0030(1)	0.3508(1)	0.2476(1)	81(3)
O1	0.068(2)	0.407(1)	0.087(1)	237(44)
O2	0.913(2)	0.404(1)	0.408(1)	300(49)
O3	0.792(2)	0.464(1)	0.206(1)	220(43)
O4	0.171(3)	0.481(2)	0.284(1)	345(52)
O11	0.817(3)	0.101(2)	0.421(1)	330(50)
O12	0.183(3)	0.054(2)	0.420(2)	421(59)
O13	0.068(2)	0.228(1)	0.351(1)	214(42)
O14	0.067(3)	0.185(2)	0.555(2)	662(76)
O21	0.208(2)	0.208(1)	0.774(1)	225(43)
O22	0.823(2)	0.178(1)	0.750(1)	229(44)
O23	0.971(3)	0.288(1)	0.906(1)	320(50)
O24	0.974(3)	0.350(2)	0.710(1)	367(53)
O31	0.032(2)	0.951(1)	0.815(1)	310(50)
O32	0.028(2)	0.768(1)	0.865(1)	293(5)
O33	0.255(3)	0.888(2)	0.978(2)	514(6)
O34	0.890(3)	0.898(2)	0.991(2)	540(67)

The oxygen atoms were refined isotropically. Standard deviations are given in parentheses.

Table 3
Bond lengths (in pm)

Bond lengths					
Re(1)–O(11)	170 (2)	Re(2)–O(21)[a]	172 (2)	Re(3)–O(31)	172 (2)
Re(1)–O(12)	173 (2)	Re(2)–O(22)[a]	174 (2)	Re(3)–O(32)[a]	170 (2)
Re(1)–O(13)[a]	172 (2)	Re(2)–O(23)	170 (2)	Re(3)–O(33)	169 (2)
Re(1)–O(14)	167 (3)	Re(2)–O(24)	171 (2)	Re(3)–O(34)	164 (2)
Yb–O(1)	235 (2)	Yb–O(4)	233 (2)	Yb–O(22)	238 (2)
Yb–O(2)	234 (2)	Yb–O(13)	231 (2)	Yb–O(32)	230 (2)
Yb–O(3)	232 (2)	Yb–O(21)	237 (2)		

[a] Indicates the distance from Re to the coordinating oxygen atoms. Standard deviations are given in parentheses.

Nonius CAD 4 four circle diffractometer. The unit cell was obtained by least-squares fitting of the setting of 25 reflections automatically centered in the range $10.6° < 2\theta < 22.6°$. The structure was solved by direct methods in the space group $P2_1/n$ and subsequently refined by least-squares methods using the SHELX 93 and SHELX 97 program system [12]. Some crystallographic details are given in Table 1. The final parameters are listed in Table 2. Selected bond lengths are listed in Table 3.

Yb_2O_3 (99.99%, Aldrich) was added stepwise to 10 mL of a concentrated solution of $HReO_4$ until it reached pH = 7. Excess of Yb_2O_3 was filtered off and washed with water. The filtrate was concentrated at 60°C. Immediately after the appearance of the first crystals the solution was left to concentrate through evaporation at room temperature. After a few days, single crystals were obtained.

2.2. Structure determination

A transparent prism-like crystal of $Yb(ReO_4)_3(H_2O)_4$ was sealed in a glass capillary and mounted on an Enraf

3. Results and discussion

3.1. Crystal growth and crystal structure

$Yb(ReO_4)_3(H_2O)_4$ crystallizes in space group $P2_1/n$, with four formula units in the unit cell. It was remarkable to note that a previously known ytterbium perrhenate, also a tetrahydrate, crystallized in the triclinic system [13,14]. We have found out that this difference in crystal structure is due to the different temperatures used during the crystallization process.

Thus, in contrast to the room temperature crystallization used for the triclinic form, the initial crystal seeds of the present polymorph nucleated and were initially grown at 60°C, after which they kept growing at room temperature. This subtle difference in nucleation temperature results in a substantial difference in crystal structure as it is described below.

Similarly to what is found in the triclinic modification of this compound (crystallized at room temperature) [13,14], in the title monoclinic modification, the ytterbium ions are eightfold coordinated in a distorted cubic antiprism. Nevertheless, in the structure we present here, the antiprism coordination is formed by four ReO_4 tetrahedra and four H_2O molecules (Fig. 1), whereas in the previously reported modification, five ReO_4 tetrahedra and three water molecules constitute the coordination sphere of the ytterbium ions.

Two crystallographically independent perrhenate anions act as terminal ligands, whereas the other two (symmetry-related) ReO_4^- tetrahedra (Re2, Re2') connect the ytterbium ions along [100], forming chains of global formula $\frac{1}{\infty}[Yb(ReO_4)_{2/2}(ReO_4)_2(H_2O)_4]$ (Fig. 2). This structural feature is one of the main differences with the triclinic modification of this compound. The latter is characterized by the condensation of units $[(ReO_4)_{2/2}(ReO_4)(H_2O)_4Yb(\mu\text{-}ReO_4)_2Yb(H_2O)_4(ReO_4)(ReO_4)_{2/2}]$, where each Yb cation is coordinated by four bridge perrhenates, one terminal ReO_4 and four water molecules. This repeating unit contains two Yb ions bridged by two ReO_4 tetrahedra. Each of the Yb is in turn connected with other repeating units through two other ReO_4^- anions

Comparing the structure of the Yb(III) perrhenate with those of the larger rare-earth perrhenates, it can be seen that the smaller ionic radii of Yb(III) does affect the coordination number as well as the connectivity of the polyhedron in the solid. The structure changes from three-dimensional networks like $\frac{3}{\infty}[La(ReO_4)_3(ReO_4)_{2/2}(ReO_4)_{3/3}(H_2O)_3]$ and $\frac{3}{\infty}[Eu(ReO_4)_{6/2}(H_2O)_3]$ to the chain already described for Yb.

Like in the perrhenates of the larger rare-earth cations, the ReO_4^- tetrahedra are only slightly distorted
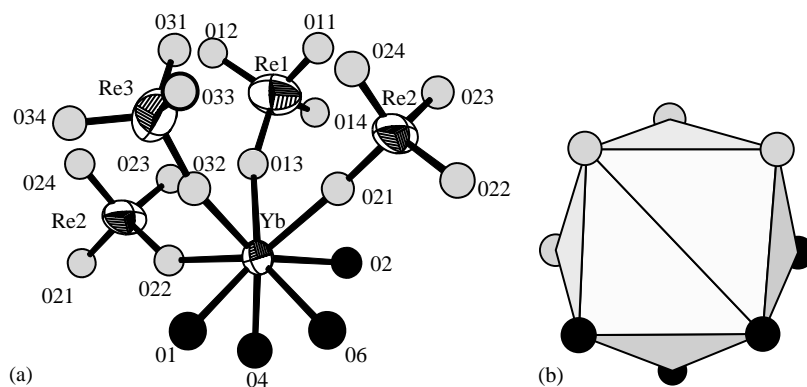

Fig. 1. (a) Coordination around Yb atom. Thermal ellipsoids for metal atoms are drawn with 99.9% probability and oxygen atoms are represented isotropically. Atomic labeling according to Table 2. (b) Coordination polyhedron around Yb. Black circles represent water molecules and gray circles represent (ReO_4) groups.
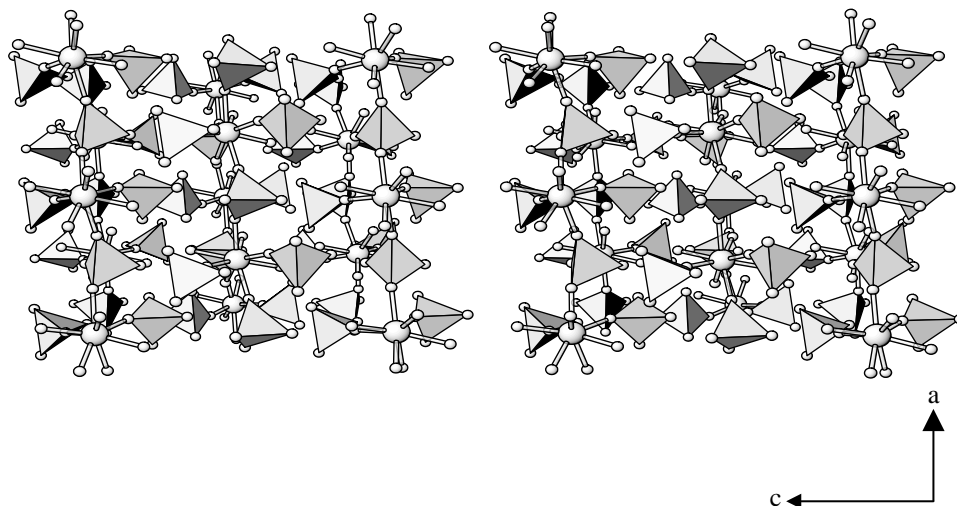

Fig. 2. Polyhedral representation of $Yb(ReO_4)_3(H_2O)_4$ along [010].

with the mean bond length $\bar{d}$ (Re–O) = 171 pm. This value corresponds well with that observed in the tetraoxorhenate(VII) complexes of the divalent ions of the first row transition metals [1–7] and in the salt-like alkali metal tetraoxorhenates(VII) $RbReO_4$ and $CsReO_4$ [15,16]. The Re–O distances to the coordinating oxygen atoms do not exhibit any significant elongation indicating an ionic interaction between the ReO_4^- ligand and the central Yb atom.

The Yb–OH_2 bond lengths are in the narrow range of about 232(2)–235(2) pm. The bond lengths Yb–$OReO_3$ are not very different, ranging from 230(2)–238(2) pm with a mean value $\bar{d}$(Yb–O) = 234 pm.

Distances d(O–O) = 275 occur in the intermolecular region between the oxygen atoms of the water ligands and oxygen atoms of the ReO_4 ligands of neighboring chains. These values are in the range of the mean O–O distances observed in ice [17]. Although it was not possible to refine the hydrogen positions with our data, it can be concluded that the chains are held together in the solid by means of hydrogen bonding.

3.2. Magnetic behavior of $Yb(ReO_4)_3(H_2O)_4$

Magnetic measurements were carried out with a Quantum Design SQUID magnetometer, in the temperature range of 5–300 K, under a magnetic field of 5000 G. The data were corrected for the corresponding atomic diamagnetic contributions according to Selwood data [18]. As illustrated in Fig. 3 the magnetic data show two regions, a high-temperature range ($90 K < T < 300 K$) where it follows a Curie–Weiss law with $\theta = -42 K$ and a low-temperature range ($< 40 K$) with a Curie law (θ approximately 0). The μ_{eff} at room temperature (calculated as $(8\chi T)^{1/2}$) lies very close to the calculated Van Vleck's value of 4.5 μ_B, for the free Yb^{3+} ion [19]. At low-temperature μ_{eff} is close to 3 μ_B. This magnetic behavior is consistent with isolated Yb^{3+} ions [19] and the lack of any antiferromagnetic interaction between the ytterbium ions, which in turn is consistent with the essentially ionic interaction between ytterbium ions and ReO_4^- ligands.

3.3. Thermogravimetric analysis

Thermogravimetric (TG) measurements were carried out to study the thermal stability as well as to evaluate the possibility to use the new compound in the synthesis of ternary oxides of rhenium with rare-earth elements. The sample was heated up to 1450 K under argon atmosphere at a rate of 5 K min^{-1}. Under these experimental conditions the dehydration proceeds in two steps below 400 K, with the formation of an intermediate dihydrate in the first step (see Fig. 4). The decomposition also takes place in two steps. In the first one $Yb(ReO_4)_3$ decomposes into a compound consistent
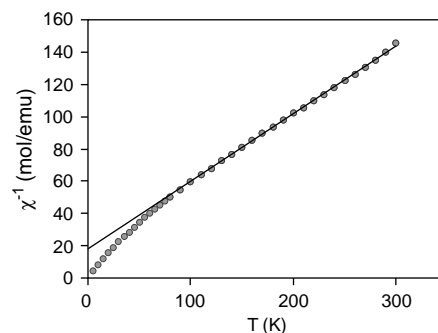

Fig 3. Plot of the inverse of magnetic susceptibility versus temperature for the title compound. The straight line is a linear regression ($R^2 = 0.9996$) to the data between 90 K and room temperature and yields a value of $\theta = -42 K$ ($\chi = C/(T + \theta)$).
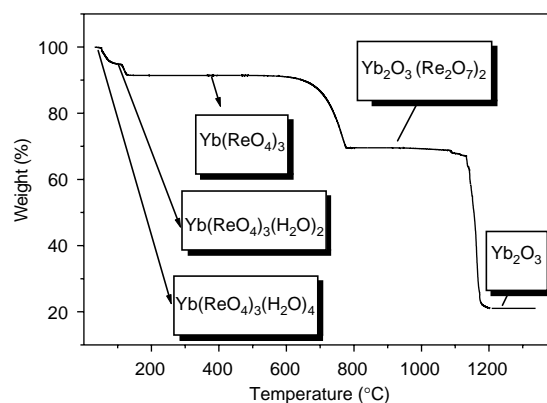

Fig. 4. Thermogravimmetry curve of $Yb(ReO_4)_3 \cdot 4H_2O$ showing the two steps of dehydration and the two steps of decomposition.

with the formula $Yb_2O_3(Re_2O_7)_2$ by losing half-mol of volatile Re_2O_7 per mol of $Yb(ReO_4)_3$. The second decomposition step takes place above 1350 K by losing of two moles of Re_2O_7 per mol of Yb_2O_3. The final solid residue was characterized as Yb_2O_3 (see Fig. 4).

Acknowledgments

References

[1] C. Mujica, K. Peters, E.-M. Peters, H.G. von Schnering, Z. Kristallogr. NCS 212 (1997) 294.

[2] C. Mujica, K. Peters, E.-M. Peters, H.G. von Schnering, Z. Kristallogr. NCS 212 (1997) 295.

[3] C. Mujica, K. Peters, E.-M. Peters, H.G. von Schnering, Z. Kristallogr. NCS 213 (1998) 10.

[4] C. Mujica, K. Peters, E.-M. Peters, H.G. von Schnering, Z. Kristallogr. NCS 213 (1998) 11.

[5] A. Butz, I. Svoboda, H. Paulus, H. Fuess, J. Solid State Chem. 115 (1995) 255.

[6] A. Butz, G. Miehe, H. Paulus, P. Strauss, H. Fuess, J. Solid State Chem. 138 (1998) 232.

[7] C. Mujica, K. Peters, E.-M. Peters, H.G. von Schnering, Z. Kristallogr. NCS 213 (1998) 229.

[8] C. Mujica, K. Peters, E.-M. Peters, H.G. von Schnering, Z. Kristallogr. NCS 212 (1998) 297.

[9] C. Mujica, J. Llanos, K. Peters, E.-M. Peters, H.G. von Schnering, J. Alloys Compds. 288 (1999) 120.

[10] C. Mujica, J. Llanos, K. Peters, E.-M. Peters, H.G. von Schnering, Bol. Soc. Chil. Quim. 45 (2000) 329.

[11] V.P. Pashonkin, V.V. Ilyukhin, N.V. Belov, Sov. Phys. Dokl. 20 (1976) 598.

[12] G. Sheldrick, Program Package SHELXTL-PLUS. Release 4.1. Siemens Analytical X-ray Instruments INC., Madison, WI 53719, USA, 1990.

[13] V.P. Mashonkin, V.V. Ilyukhin, N.V. Belov, Sov. Phys. Dokl. 19 (1975) 634.

[14] E.D. Bakhareva, M.B. Vormolomeyev, V.V. Ilyukhin, Koordinatsionnaya Khimiya 2 (1976) 1135.

[15] P. Roegner, K.-J. Range, Z. Naturforsch. B 47 (1992) 233.

[16] P. Roegner, K.-J. Range, Z. Naturforsch. B 48 (1993) 685.

[17] W.C. Hamilton, J.C. Ibers, Hydrogen Bonding in Solids, W.A. Benjamin, New York, 1968.

[18] S. Selwood, Magnetochemistry, Interscience Publishers, New York, 1956.

[19] A.T. Casey, S. Mitra, in: E.A. Boudreaux, L.N. Mulay (Eds.), Theory and Applications of Molecular Paramagnetism, Wiley, New York, 1976, pp. 309–312.